Sensor-based 3-D Pose Estimation and Control of Rotary-wing UAVs using a 2-D LiDAR

Alexandre Gomes[1], Bruno J. Guerreiro[1⋆], Rita Cunha[1], Carlos Silvestre[2,1⋆⋆], and Paulo Oliveira[3,1]

[1] Institute for Systems and Robotics (ISR/IST), LARSYS, Instituto Superior Técnico, Universidade de Lisboa, Portugal

[2] Department of Electrical and Computer Engineering, Faculty of Science and Technology, University of Macau, Taipa, Macau SAR, China

[3] Associated Laboratory for Energy, Transports, and Aeronautics (LAETA), Instituto Superior Técnico, Universidade de Lisboa, Portugal

Abstract. This paper addresses the problem of deriving attitude estimation and trajectory tracking strategies for unmanned aerial vehicles (UAVs) using exclusively on-board sensors. The perception of the vehicle position and attitude relative to a structure is achieved by robustly comparing a known pier geometry or map with the data provided by a LiDAR sensor, solving an optimization problem and also robustly identifying outliers. Building on this information, several methods are discussed for obtaining the attitude of the vehicle with respect to the structure, including a nonlinear observer to estimate the vehicle attitude on $\mathcal{SO}(3)$. A simple nonlinear control strategy is also designed with the objective of providing an accurate trajectory tracking control relative to the structure, and experimental results are provided for the performance evaluation of the proposed algorithms.

1 Introduction

Unmanned aerial vehicles (UAVs), more informally known as drones, were initially developed within a military context [3, 16], yet soon the world realized that these small vehicles could be used in tasks other than warfare, such as the inspection of infrastructures. The technological evolution has led to an increase in the demand for more and larger wind turbines, cellphone towers, and power lines, to name a few. All these large buildings and facilities are critical infrastructures that require maintenance through structural inspections and health monitoring, which can become inefficient in situations where the access is difficult, time-consuming, and often dangerous. Small vehicles such as UAVs constitute a tailor-made solution, able to navigate and track trajectories with great accuracy. While the motion control of aerial vehicles in free flight is reaching

⋆ Corresponding Author. E-mail: bguerreiro@isr.tecnico.ulisboa.pt.

⋆⋆ C. Silvestre is also on leave from the Department of Electrical and Computer Engineering, Instituto Superior Técnico, Universidade de Lisboa, Portugal.

its maturity, new challenges that involve interaction with the environment are being embraced. Using local sensors, such as inertial measurement units (IMUs) and light detection and ranging (LiDAR) sensors, some quantities required for control tasks can be obtained depending solely on the vehicle. Having a GPS enables these vehicles to fly autonomously, a feature that can become compromised in the vicinity of large infrastructures, as the GPS signal can be easily occluded by these structures. This paper aims to take the interaction with the environment one step further, using information from the vehicle's surroundings.

Using LiDARs for self localization in GPS-denied environments is by now an ubiquitous and mandatory technology in mobile robots [15], and more applications of this type of sensor are emerging for UAVs, as in [8] or [6]. In comparison with video cameras, also used in visual structure from motion algorithms [17], LiDARs offer better depth resolution, range, and horizontal field of view at the cost of lower horizontal and vertical resolution. Building on the work presented in [7, 4], this work extends the relative pose of the vehicle to include its attitude, allowing a full 3-D structure dependent trajectory to be defined, provided that a known geometry in the environment is present (such as a pier). For detecting the geometric primitives necessary for relative pose estimation, several approaches are available, either for circular-like piers [14] or for planar-wise structures [11], where the edges detected in the environment are the foundations to obtain the 3-D attitude estimate. Given the resolution limitations of the considered LiDARs, this work assumes the existence of a rectangular section pier, for which one or two faces are always visible to the LiDAR. An edge detection strategy is proposed, and based on simple geometric properties, the variations of the detected edges can be used to extract a pair of 3-D vectors, in the vehicle and world frames. With these vector pairs, several attitude estimation algorithms can be used, such as the solution to the well-known Wahba's problem [10], or more evolved nonlinear filters [1]. This paper also proposes a nonlinear filter to compute the rotation matrix describing the motion of a vehicle based on the fusion of LiDAR and IMU measurements. Finally, the motion control design yields a trajectory tracking controller solely based on local sensory information, therefore providing a relative positioning solution for GPS-denied environments.

The paper is organized as follows. Section 2 discusses the edge detection approach, combining algorithms such as the Split & Merge and least square fitting. Section 3 designs several methods to obtain the vehicle's attitude from the detected edges. Next, Section 4 discusses the control strategies developed for trajectory tracking, whereas Section 5 compares the attitude estimation algorithms using experimental data and validates the control strategy with experimental trials. Finally, some concluding remarks are offered in Section 6.

2 Environment Perception

Detecting a structure and obtaining the necessary information to determine the vehicle's attitude greatly depends on the knowledge of its geometry. This paper considers piers with a rectangular section, where the LiDAR can see one or two

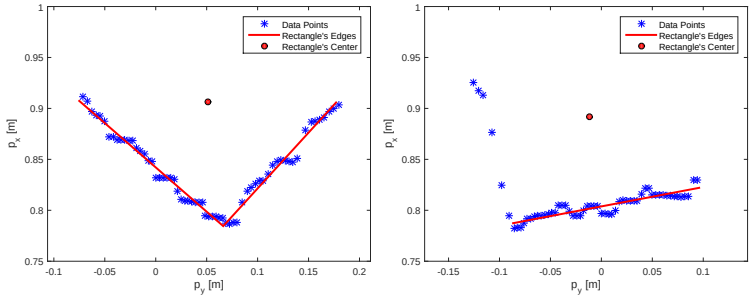

Fig. 1. Cuboid pier detection during an experiment: 2 edges (left) or 1 edge (right).

faces of the pier, depending on its relative pose. The intersection of this sensor's plane with these faces will result in two straight lines, hereafter simply referred as edges.

The idea behind attitude determination is that a specific movement, in roll or pitch, has an impact on both the edges' lengths and angle between them (further details can be found in [4]). The first step involves identifying how many edges the vehicle is encountering at each moment, for which a strategy based on the Split & Merge algorithm was developed [11, 12]. The basic principle to determine if the LiDAR is detecting one or more edges is to compare a given threshold with the perpendicular distance from each LiDAR measurement point $\mathbf{p}_i = \begin{bmatrix} x_i & y_i & z_i \end{bmatrix}^T \in \mathbb{R}^3$ to a line. This distance can be defined as $e_i = \mathbf{p}_i^T \mathbf{n} + c$, where $\mathbf{n} = \begin{bmatrix} n_x & n_y & n_z \end{bmatrix}^T \in \mathbb{S}^2$ is the unit vector normal to the line, as $\mathbb{S}^2$ denotes the unit sphere in $\mathbb{R}^3$, and c is the offset from the origin. Additional deciding factors are also used, taking into account the number of LiDAR measurements supporting each edge, the geometry of the edges relative to the existing knowledge about them, rejecting outliers using the average distance between consecutive data points, among others. Fig. 1 presents the output of this detection strategy, either with both edges clearly visible, or in a transition stage, where the algorithm helps deciding how many edges should be considered in the next phases.

With this rough estimate of each edge, a least squares line fitting can be used to further improve these estimates. The problem at hand is in the form

$$\begin{aligned} &\min_{c,\mathbf{n}\in\mathbb{S}^2} \sum_{i=1}^{N} e_i^2 \\ &s.t. \;\; e_i = c + \mathbf{p}_i^T \mathbf{n} \;, \forall_{i=1,\dots,N} \end{aligned}$$

also found in [5], which after some mathematical manipulations, can be determined by the singular value decomposition (SVD) of a reduced problem. A reduced space Hough transform was also considered [13], but as it yielded similar results at a much higher computational cost, the option was to use exclusively the LS fitting strategy.

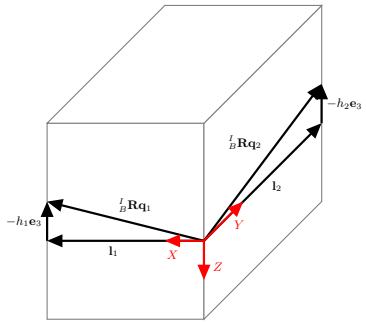

Fig. 2. Decomposition of the edges in $\{E\}$.

The following step involves the computation of the edge lengths, or equivalently, the boundary points of each edge, denoted as start point $\mathbf{p}_{s_i} \in \mathbb{R}^3$ and end point $\mathbf{p}_{e_i} \in \mathbb{R}^3$. At this stage, it is important to define the reference frames used in the remaining of the paper, the first being the Earth-fixed frame $\{E\}$, which is considered to be the local tangent plane with the north east down (NED) convention. There is also the body frame $\{B\}$, with the origin at the vehicle's center of mass, the x-axis pointing forward, and the z-axis pointing downward along its vertical axis, whereas an intermediate horizontal frame $\{H\}$ is also useful, which can be seen as a projection of $\{B\}$ on the xy-plane of $\{E\}$. Thus, the normed direction of each edge can be represented by a vector $\mathbf{q}_i = \begin{bmatrix} q_{xi} & q_{yi} & q_{zi} \end{bmatrix}^T \in \mathbb{R}^3$, expressed in $\{B\}$, such that $\mathbf{q}_i = \mathbf{p}_{e_i} - \mathbf{p}_{s_i}$.

The representation of the edges in $\{E\}$ is also fundamental, as they can be related through the rotation matrix from $\{B\}$ to $\{E\}$, denoted by ${}^{E}_{B}\mathbf{R}$ or simply as $\mathbf{R}$, according to ${}^{E}\mathbf{q}_i = {}^{E}_{B}\mathbf{R}\,\mathbf{q}_i$. As illustrated in Fig. 2, their projection in the xy-plane of this reference frame corresponds to the section of the pier and can be defined as $\mathbf{l}_i \in \mathbb{R}^3$, with $L_i := \|\mathbf{l}_i\|$ for $i = 1, 2$. The z coordinate in frame $\{E\}$, represented by h_i, is directly linked to the attitude of the vehicle, resulting in ${}^{E}\mathbf{q}_i = \mathbf{l}_i \pm h_i\mathbf{e}_3$, where $\mathbf{e}_3 = \begin{bmatrix} 0 & 0 & 1 \end{bmatrix}^T$.

Knowing the dimensions of the pier, either from the initial LiDAR profiles or from a known map, the z coordinate can be obtained using $h_i^2 = \|\mathbf{q}_i\|^2 - L_i^2$ from the measured edges in $\{B\}$ and the known edge lengths, which are independent of the reference frame. Further using the cross product of both edges, to account for the angle between them, leads to the following optimization problem

$$\begin{aligned} \min_{h_1^2, h_2^2 \in \mathbb{R}_0^+} \quad & \sum_{i=1}^{3} \varepsilon_i^2 \\ s.t. \quad & \varepsilon_i = h_i^2 - \|\mathbf{q}_i\|^2 + L_i^2 \;\forall_{i=1,2} \\ & \varepsilon_3 = h_1^2\, L_2^2 + h_2^2\, L_1^2 - \|\mathbf{S}(\mathbf{q}_1)\mathbf{q}_2\|^2 + L_1^2\, L_2^2 \end{aligned}$$

where $\mathbf{S}(.)$ denotes the skew-symmetric matrix, such that $\mathbf{S}(\mathbf{a})\mathbf{b}$ represents the cross product $\mathbf{a} \times \mathbf{b}$, for some vectors $\mathbf{a}, \mathbf{b} \in \mathbb{R}^3$. The above problem implies

there is ambiguity in the sign of each h_i, which can be solved through continuity, by choosing the closest value to the previous one, assuming there are no swift movements around leveled flight.

3 Pose Estimation

This section builds on the previous detection strategies to propose several methods capable of accurately extracting a partial or the full attitude of the vehicle. The first approach is to obtain the vehicle's rotation about the z-axis, assuming full knowledge about the remaining angular motions, as the information provided by a simple IMU is usually sufficient to obtain the roll and pitch angles. On the other hand, two additional strategies are presented to compute the 3-D attitude of the vehicle from LiDAR data, either considering a closed-form solution to the Wahba's problem or a nonlinear attitude filter. Obtaining the relative position of the vehicle is straightforward when either one or two edge measurements are available and the geometry of the pier is known, for which it omitted from this discussion.

3.1 Yaw Motion

As the roll and pitch angles can be obtained fairly easy and accurately using accelerometers and gyroscopes, at low acceleration motions, a better estimate of the yaw angle ψ can be obtained using LiDAR measurements, independently of possible distortions on the Earth magnetic field. Thus, the LiDAR measurements can be projected into $\{H\}$ using ${}^{H}\mathbf{p}_i = \mathbf{\Pi}_{\mathbf{e}_3} {}^{H}_{B}\mathbf{R}\, \mathbf{p}_i$ for $i = 1, \ldots, N$, where $\mathbf{\Pi}_{\mathbf{e}_3} = \mathrm{diag}\,(1, 1, 0)$ and ${}^{H}_{B}\mathbf{R}$ depends only on the roll and pitch angles.

As this projection leaves the yaw angle ψ as the only remaining degree of freedom, a new optimization problem can be defined to fit simultaneously two orthogonal edges to the data, after the Split & Merge algorithm, yielding

$$\begin{aligned} \min_{c_1, c_2, \mathbf{n} \in \mathbb{S}^1} \quad & \sum_{i=1}^{N_1+N_2} e_i^2 \\ s.t. \quad & e_i = c_1 + {}^{H}\mathbf{p}_i^T\, \mathbf{T}_1\, \mathbf{n}\,, i = 1, \ldots, N_1 \\ & e_i = c_2 + {}^{H}\mathbf{p}_i^T\, \mathbf{T}_2\, \mathbf{n}\,, i = N_1 + 1, \ldots, N_1 + N_2 \end{aligned}$$

where $\mathbf{T}_1\, \mathbf{n} = \begin{bmatrix} n_x & n_y & 0 \end{bmatrix}^T$, and $\mathbf{T}_2\, \mathbf{n} = \begin{bmatrix} -n_y & n_x & 0 \end{bmatrix}^T$. With this approach, the estimation error of the relative heading can be reduced, as the data points of both edges now contribute to an unified objective. The estimated edges in $\{E\}$ can then be computed using ${}^{E}\mathbf{q}_i = {}^{E}_{H}\mathbf{R}\, {}^{H}\mathbf{q}_i$, while the yaw angle estimate can be simply computed using $\hat{\psi} = \mathrm{atan2}\left({}^{E}q_{yi}, {}^{E}q_{xi}\right) + \psi_{0i}$, where atan2 is the 4 quadrant inverse tangent function and ψ_{0i} is the relative yaw difference for edge i.

3.2 3-D Attitude Estimation

Considering the motion capabilities of a rotary-wing UAV, with the intrinsic limitations of using LiDAR measurements relative to a pier, this section considers the estimation of the 3-D attitude of the vehicle relative to the infrastructure. The information provided by an IMU is a product of the combination of three types of sensors: accelerometers, gyroscopes, and magnetometers. The data provided by the accelerometers, for low vehicle acceleration motions, has a direct connection with the attitude of the vehicle relative to the earth surface, but it cannot be used to describe the attitude about the z-axis. The gyroscopes' data can act as a complement, bearing in mind that the integration of angular velocity over time accumulates errors with ever growing significance. The magnetometers can compensate some of these errors, but are highly susceptible to drifts and environmental disturbances, in particular when close to infrastructures.

A commonly used approach to obtain 3-D attitude from vector measurements is the solution to the Wahba's problem, estimating the proper orthogonal matrix ${}^{B}_{E}\mathbf{R}$ by solving the minimization problem

$$\min_{{}^{B}_{E}\mathbf{R}\in\mathcal{SO}(3)} \quad \frac{1}{2}\sum_{i=1}^{n_{obs}} w_i \left\| \mathbf{o}_i - {}^{B}_{E}\mathbf{R}\, {}^{E}\mathbf{o}_i \right\|^2$$

where ${}^{E}\mathbf{o}_i$ and $\mathbf{o}_i$, for $i = 1, \ldots, n_{obs}$, denote the normalized vector measurements represented respectively in $\{E\}$ and $\{B\}$, denoted in matrix form as ${}^{E}\mathbf{O}$ and $\mathbf{O}$ with columns as the individual vector measurements, whereas w_i are positive weights associated with each individual measurement and n_{obs} is the total number of observations.

One solution to this problem can be traced back to [10], considering that the measurements are free of errors, implying that the true rotation matrix ${}^{B}_{E}\mathbf{R}$ is the same for all measurements, yielding the closed-form solution

$${}^{B}_{E}\hat{\mathbf{R}} = \mathbf{U}\,\mathrm{diag}\left(1, 1, \det(\mathbf{U})\det(\mathbf{V})\right)\mathbf{V}^T$$

where $\mathbf{U}$ and $\mathbf{V}$ are orthogonal matrices, obtained from the SVD of matrix $\mathbf{H} = \sum_{i=1}^{n_{obs}} w_i\, \mathbf{o}_i\, {}^{E}\mathbf{o}_i^T$. While most of the times there are two LiDAR-based edges that fully define the attitude of the vehicle, an ambiguity arises when only one edge is visible. To avoid this, the acceleration vector can be used, assuming that the vehicle's acceleration is negligible relative to Earth's gravity. With that in mind, the extended observation matrices can be defined as $\mathbf{O} = \begin{bmatrix}\mathbf{q}_1 & \mathbf{q}_2 & \mathbf{a}\end{bmatrix}$, where the additional observation is the normalized acceleration vector and a similar matrix ${}^{E}\mathbf{O}$ can be defined. This can also be translated into the following assumption.

Assumption 1 *There are at least two non-zero and non-collinear vector measurements,* $\mathbf{o}_i$ *and* $\mathbf{o}_j$*, with* $i \neq j$*.*

Another approach is to design a rotation matrix observer that further uses the gyroscopes information to drive the filter. To this end, consider the kinematics of ${}^{B}_{E}\mathbf{R}$, given by ${}^{B}_{E}\dot{\mathbf{R}} = -\mathbf{S}(\boldsymbol{\omega})\,{}^{B}_{E}\mathbf{R}$, where $\boldsymbol{\omega}$ is the angular velocity. An

observer for ${}^{B}_{E}\mathbf{R}$ replicates this structure, as ${}^{B}_{E}\dot{\hat{\mathbf{R}}} = -\mathbf{S}(\hat{\boldsymbol{\omega}}){}^{B}_{E}\hat{\mathbf{R}}$, where $\hat{\boldsymbol{\omega}}$ is yet to be determined. As such, the error between the true rotation matrix and its estimate can be defined as $\tilde{\mathbf{R}} = {}^{B}_{E}\mathbf{R}\,{}^{B}_{E}\hat{\mathbf{R}}^{T}$, resulting in the error dynamics

$$\dot{\tilde{\mathbf{R}}} = \tilde{\mathbf{R}}\,\mathbf{S}(\hat{\boldsymbol{\omega}}) - \mathbf{S}(\boldsymbol{\omega})\,\tilde{\mathbf{R}} \tag{1}$$

for which the stability of the equilibrium point $\tilde{\mathbf{R}} = \mathbf{I}_3$ is stated in the following result.

Theorem 1. *Considering the error dynamics in* (1)*, let* $\hat{\boldsymbol{\omega}}$ *be defined as*

$$\hat{\boldsymbol{\omega}} = \boldsymbol{\omega} + k_{obs} \sum_{i=1}^{n_{obs}} \mathbf{S}(\mathbf{o}_i)\tilde{\mathbf{R}}^{T}\mathbf{o}_i \tag{2}$$

with $k_{obs} > 0$*. Under Assumption 1, the equilibrium point* $\tilde{\mathbf{R}} = \mathbf{I}_3$ *is almost globally asymptotically stable.*

Proof. For the proof outline, let the candidate Lyapunov funcion be defined as

$$V(\tilde{\mathbf{R}}) = \operatorname{tr}\left(\mathbf{I}_3 - \tilde{\mathbf{R}}\right) \tag{3}$$

where $\mathbf{I}_3$ is the identity matrix. It can easily be seen that this function is positive definite and vanishes at the equilibrium point, as $V(\tilde{\mathbf{R}}) > 0$ for all $\tilde{\mathbf{R}} \in \mathcal{SO}(3) \setminus \mathbf{I}_3$ and $V(\mathbf{I}_3) = 0$. After replacing (2) and some algebraic manipulation, the derivative of (3) can be written as

$$\dot{V}(\tilde{\mathbf{R}}) = -\frac{k_{obs}}{2} \sum_{i=1}^{n_{obs}} \left\| (\mathbf{I}_3 - \tilde{\mathbf{R}}^2)\mathbf{o}_i \right\|^2 .$$

Considering Assumption 1, it can be seen that $\dot{V}(\tilde{\mathbf{R}}) \leq 0$ for all $\tilde{\mathbf{R}} \in \mathcal{SO}(3)$ and that $\dot{V}(\tilde{\mathbf{R}}) = 0$ if and only if $\tilde{\mathbf{R}} = \mathbf{I}_3$ and $\tilde{\mathbf{R}} = \operatorname{rot}(\pi, \mathbf{n})$, for all $\mathbf{n} \in \mathbb{S}^2$, where the notation $\operatorname{rot}(\theta, \mathbf{n})$ denotes a rotation about the unitary vector $\mathbf{n}$ of an angle θ. As such, it can be shown that the error system is almost globally asymptotically stable, meaning that the region of attraction covers all of $\mathcal{SO}(3)$, except for a zero measure set of initial conditions, following the approach in [2, 1]. □

The integration of angular velocity measurements directly from the gyroscopes usually suffers from drift over time. In this event, these measurements $\boldsymbol{\omega}_m$ are corrupted by a measurement bias $\mathbf{b}_\omega$ according to $\boldsymbol{\omega}_m = \boldsymbol{\omega} + \mathbf{b}_\omega$, and the convergence of the observer to the true rotation matrix cannot be guaranteed without further modifications. Nonetheless, it can be shown that the derivative of the Lyapunov function is negative definite as long as $|\sin(\theta)| > \|\mathbf{b}_\omega\| / K_{obs}\lambda_{min}(\mathbf{P})$, where θ is the angle of the error matrix $\tilde{\mathbf{R}}$ in the angle-axis representation and $\mathbf{P} = \operatorname{tr}\left(\mathbf{O}\mathbf{O}^T\right)\mathbf{I}_3 - \mathbf{O}\mathbf{O}^T$ is a positive definite matrix, as Assumption 1 ensures that $\lambda_{min}(\mathbf{P}) > 0$. Thus, in the presence of a sufficiently small angular velocity bias, the estimation error can be shown to be ultimately bounded [9]. A preliminary experimental evaluation of the combined detection and estimation strategies is presented in Section 5.

4 Trajectory Tracking Control

This section addresses the combination of the detection and estimation strategies and the design of controllers, aiming at tracking a trajectory defined relatively to a structure using only an IMU and a 2-D LiDAR. A nonlinear position controller is considered, for which the simplification of the force balance that describes the vehicle can be defined by the error dynamics

$$\begin{cases} \dot{\tilde{\mathbf{p}}} = {}^{E}\dot{\mathbf{p}} - {}^{E}\dot{\mathbf{p}}_d = {}^{E}\mathbf{v} - {}^{E}\mathbf{v}_d \\ \dot{\tilde{\mathbf{v}}} = {}^{E}\dot{\mathbf{v}} - {}^{E}\dot{\mathbf{v}}_d = g\mathbf{e}_3 - \frac{T}{m}\mathbf{r}_3 - {}^{E}\dot{\mathbf{v}}_d \\ \dot{\tilde{\mathbf{r}}}_3 = \dot{\mathbf{r}}_3 - \dot{\mathbf{r}}_{3_d} = -\mathbf{S}(\mathbf{r}_3)\mathbf{R}^T\mathbf{\Pi}_{\mathbf{e}_3}\boldsymbol{\omega} - \dot{\mathbf{r}}_{3_d} \end{cases} \tag{4}$$

where m is the vehicle mass, g is the gravitational acceleration, ${}^{E}\mathbf{p}$, ${}^{E}\mathbf{v}$, $\mathbf{r}_3$, and T are respectively the vehicle's position, velocity, third column of the rotation matrix $\mathbf{R} = {}^{E}_{B}\mathbf{R}$, and the thrust input, whereas ${}^{E}\mathbf{p}_d$, ${}^{E}\mathbf{v}_d$, $\mathbf{r}_{3_d}$, and T_d are their respective desired values. In these error dynamics, only the first two elements of the angular velocity are used as inputs, denoted as $\mathbf{\Pi}_{\mathbf{e}_3}\boldsymbol{\omega} = \begin{bmatrix}\omega_x & \omega_y & 0\end{bmatrix}^T$, leaving the angular motion about the vehicle's z-axis as an extra degree of freedom. An alternative input $\bar{\boldsymbol{\omega}}$ can also be defined for simplicity as $\mathbf{\Pi}_{\mathbf{e}_3}\boldsymbol{\omega} = -\mathbf{R}\mathbf{S}(\mathbf{r}_3)^2\bar{\boldsymbol{\omega}}$.

The approach to stabilize this nonlinear system consists of first stabilizing the position and velocity outer-loop driven by $\mathbf{r}_{3_d}$ and T_d, introducing a new state $\mathbf{x} = \begin{bmatrix}\tilde{\mathbf{p}}^T & \tilde{\mathbf{v}}^T\end{bmatrix}^T$, and then using backstepping techniques to drive the attitude and trust to the desired values using the vehicle thrust and part of the angular velocity vector. The following result provides the conditions for asymptotic stability of the closed-loop system, assuming full state feedback.

Theorem 2. *Consider the error dynamics* (4)*, for which the feedback law is chosen as* $T = T_d\,\mathbf{r}_3^T\mathbf{r}_{3_d}$*,* $\mathbf{r}_{3_d} = \frac{m}{T_d}\mathbf{f}$*,* $T_d = m\,\|\mathbf{f}\|$*, with the alternative input* $\bar{\boldsymbol{\omega}}$ *defined as*

$$\bar{\boldsymbol{\omega}} = \frac{1}{\|\mathbf{f}\|}\mathbf{S}(\mathbf{r}_{3_d})\dot{\mathbf{f}} - \mathbf{S}(\mathbf{r}_3)\left[\frac{2T_d}{m}\left(\mathbf{P}_{12}\tilde{\mathbf{p}} + \mathbf{P}_{22}\tilde{\mathbf{v}}\right) + K_{\tilde{\mathbf{r}}_3}\tilde{\mathbf{r}}_3\right] \tag{5}$$

and $\mathbf{f} = g\mathbf{e}_3 - {}^{E}\dot{\mathbf{v}}_d + K_{\tilde{\mathbf{p}}}\tilde{\mathbf{p}} + K_{\tilde{\mathbf{v}}}\tilde{\mathbf{v}}$*,* $\dot{\mathbf{f}} = -{}^{E}\ddot{\mathbf{v}}_d + K_{\tilde{\mathbf{p}}}\dot{\tilde{\mathbf{p}}} + K_{\tilde{\mathbf{v}}}\dot{\tilde{\mathbf{v}}}$*, while* $\mathbf{P}_{12}$ *and* $\mathbf{P}_{22}$ *are constant design matrices, and* $K_{\tilde{\mathbf{r}}_3} > 0$ *is a controller gain. Then the closed-loop system is asymptotically stable.*

Proof. The proof outline for this strategy starts by defining the Lyapunov function candidate

$$V(\tilde{\mathbf{p}}, \tilde{\mathbf{v}}, \tilde{\mathbf{r}}_3) = \mathbf{x}^T\mathbf{P}\mathbf{x} + \frac{1}{2}\tilde{\mathbf{r}}_3^T\tilde{\mathbf{r}}_3$$

where $\mathbf{P}$ is a symmetric positive definite matrix. The constant design matrices $\mathbf{P}_{12}$ and $\mathbf{P}_{22}$ from 2 correspond to the blocks of $\mathbf{P}$ that are relevant to the control task, depending only on the position and linear velocity gains, $K_{\tilde{\mathbf{p}}}$ and $K_{\tilde{\mathbf{v}}}$. Using (5), after some agebraic manipulation, the derivative of this function corresponds to

$$\dot{V}(\tilde{\mathbf{p}}, \tilde{\mathbf{v}}, \tilde{\mathbf{r}}_3) = -\mathbf{x}^T\mathbf{Q}\mathbf{x} - K_{\tilde{\mathbf{r}}_3}\left\|\mathbf{S}(\mathbf{r}_3)\tilde{\mathbf{r}}_3\right\|^2 \tag{6}$$

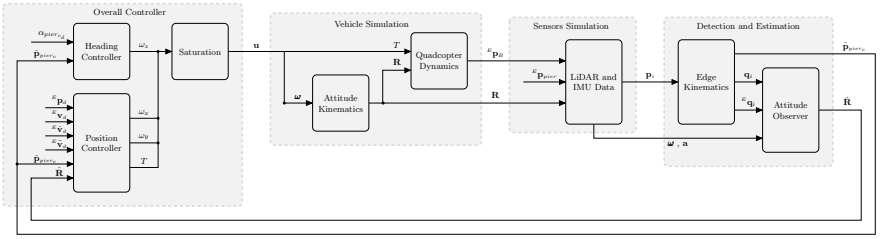

Fig. 3. Block diagram of the overall architecture.

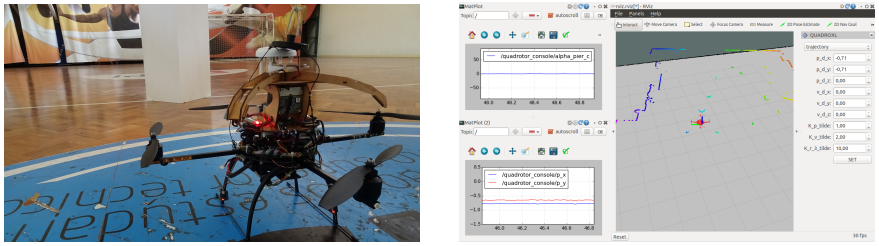

(a) Vehicle and pier (b) Control Console

Fig. 4. Experimental setup at ISR/IST.

where $\mathbf{Q}$ is a positive definite matrix. Therefore, the derivative (6) is composed of only negative definite terms leading to asymptotic stability guarantees. □

The remaining degree of freedom can be tackled using a simple heading lock controller, with the objective of maintaining a certain heading relative to the pier. A first order model of the yaw kinematics can be easily obtained using a proportional controller, resulting in a closed-loop defined as $T_{\dot{\psi}}\,\dot{\omega}_z = -\omega_z + \omega_{zd}$, where $T_{\dot{\psi}}$ is the time constant of the system. As such, the input to the system dynamics can now be defined as $\mathbf{u} = \begin{bmatrix}\omega_x\ \omega_y\ \omega_z\ T\end{bmatrix}^T$. The overall architecture of the proposed approach is presented in Fig. 3, where the controller, the simulated vehicle and LiDAR sensor, the detection, and the attitude estimation blocks can be identified.

5 Results

This section presents some experimental results regarding both the estimation algorithms and the overall controlled system. The vehicle used in these trials is based on the Mikrokopter Quadro XL, as shown in Fig. 4a, customized at ISR/IST to feature a Hokuyo LiDAR UTM30LX, a Microstrain IMU, a Gumstix mini PC, among other sensors. The detection and control algorithms were ran on board the vehicle, while a ROS-based control console was used to switch between control modes and monitor the experiments, depicted in Fig. 4b.

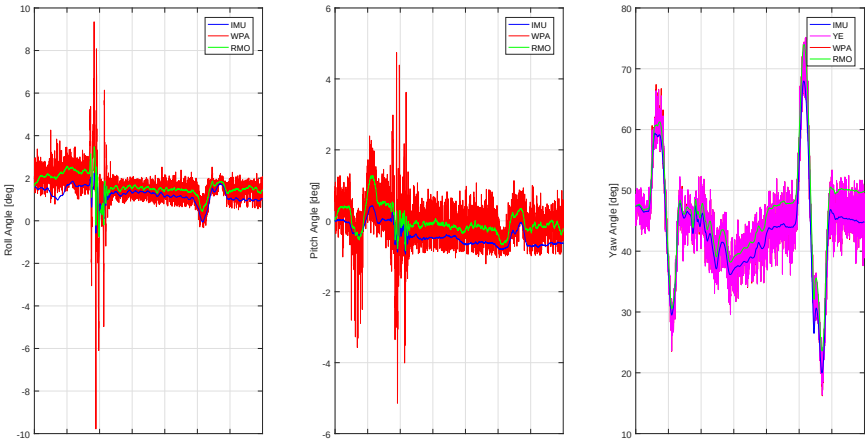

Fig. 5. Attitude determination experiments, featuring results from the IMU, the yaw estimation (YE), the Wahba's solution (WPA), and the nonlinear observer (RMO).

5.1 Estimation

Regarding the attitude estimation results, the described algorithms were tested using experimental data to assess the impact of the sensor's noise and the effectiveness of the data treatment, as shown in Fig. 5. It can be seen that both the yaw estimator (YE) and the solution to the Wahba's problem (WPA) are more prone to the measurement noise than the nonlinear rotation matrix observer (RMO) or the IMU internal filter. As such, the rotation matrix observer obtains the best results, where the attitude description obtained in the experiments can be seen as a filtered version of the previous methods, maintaining a similar proximity to the reference.

It can also be seen that the roll and pitch estimates provided by the observer have an offset relative to the attitude obtained from the IMU. This is a result from the precision of the LiDAR sensor on detecting the edges of the pier, more particularly, the end or length of each edge. It should also be noted that the oscillation in the YE and WPA methods are directly related to the uncertainties while determining the length of the edges. Moreover, all estimation methods presented a yaw motion description very similar among themselves and to what was observed in reality. In some cases not included in this paper due to space constraints, the IMU yaw measurements where severely biased, probably due to magnetic interference, while the proposed methods remained immune to this problem.

5.2 Control

The overall closed-loop system was implemented as presented in Fig. 3 and experimentally tested. The results of this preliminary experimental trial are presented

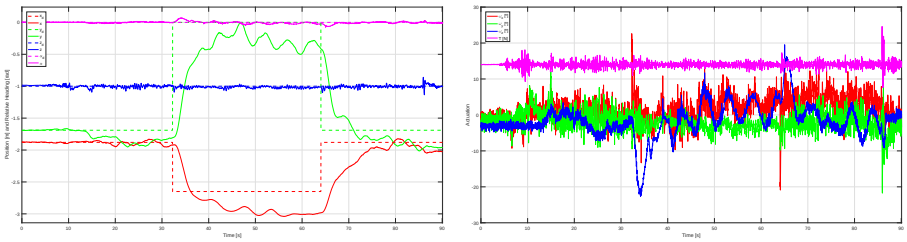

(a) Position and relative heading (b) Actuation

Fig. 6. Experimental results of the closed-loop system, using a step reference.

in Fig. 6, where the position, heading, and actuation signals are show, considering a reference with steps in position relative to the pier. It can be seen that the vehicle is able to track the reference with fair accuracy, although there is still margin for gain adjustment towards a more accurate trajectory tracking. At the same time, the vehicle actively maintains the relative heading pointing towards the pier, even when the position of the vehicle switches between two points.

6 Concluding Remarks

This paper proposes a solution to the problem of laser-based control of rotary-wing UAVs, considering the entire process comprising the acquisition and treatment of the sensor's measurements, the development of methods to compute the relevant quantities to describe the motion of the vehicle, and the design and implementation of stable and effective observers and controllers within the scope of Lyapunov stability methods. The proposed algorithms where tested in preliminary experimental trials, allowing to validate their effective applicability to the envisioned scenarios. Future work will focus on further experimental tests of the trajectory tracking controller and attitude observer, as well as in the development of more reliable, robust, and stable observers and path-following controllers.

Acknowledgments

This work was partly funded by the Macao Science and Technology Development Fund (FDCT) through Grant FDCT/048/2014/A1, by the project MYRG2015-00127-FST of the University of Macau, by LARSyS project FCT:UID/EEA/-50009/2013, and by the European Union's Horizon 2020 programme (grant No 731667, MULTIDRONE). The work of Bruno Guerreiro was supported by the FCT Post-doc Grant SFRH/BPD/110416/2015, whereas the work of Rita Cunha was funded by the FCT Investigator Programme IF/00921/2013. This publication reflects the authors' views only, and the European Commission is not responsible for any use that may be made of the information it contains. The

authors express their gratitude to the DSOR team, in particular to B. Gomes, for helping with the experimental trials.

References

1. Brás, S., Cunha, R., Silvestre, C.J., Oliveira, P.J.: Nonlinear attitude observer based on range and inertial measurements. Control Systems Technology, IEEE Transactions on **21**(5), 1889–1897 (2013)
2. Cunha, R.: Advanced motion control for autonomous air vehicles. Ph.D. thesis, Instituto Superior Técnico, Universidade Técnica de Lisboa, Lisbon, Portugal (2007)
3. Franke, U.E.: Civilian drones: Fixing an image problem? ISN Blog, ETH Zurich (2015). URL http://isnblog.ethz.ch/security/civilian-drones-fixing-an-image-problem
4. Gomes, A.: Laser-based control of rotary-wing UAVs. Master's thesis, Aerospace Eng., Instituto Superior Técnico (2015)
5. Groenwall, C.A., Millnert, M.C.: Vehicle size and orientation estimation using geometric fitting. In: Aerospace/Defense Sensing, Simulation, and Controls, pp. 412–423. International Society for Optics and Photonics (2001)
6. Guerreiro, B.J., Batista, P., Silvestre, C., Oliveira, P.: Globally asymptotically stable sensor-based simultaneous localization and mapping. IEEE Transactions on Robotics **29**(6) (2013). DOI https://doi.org/10.1109/TRO.2013.2273838
7. Guerreiro, B.J., Silvestre, C., Cunha, R., Cabecinhas, D.: Lidar-based control of autonomous rotorcraft for the inspection of pier-like structures. IEEE Transactions in Control Systems Technology (2017). DOI https://doi.org/10.1109/TCST.2017.2705058
8. He, R., Prentice, S., Roy, N.: Planning in information space for a quadrotor helicopter in a GPS-denied environment. In: IEEE International Conference on Robotics and Automation, pp. 1814–1820. Pasadena, CA, USA (2008)
9. Khalil, H.K., Grizzle, J.: Nonlinear systems, vol. 3. Prentice hall New Jersey (1996)
10. Markley, F.L.: Attitude determination using vector observations and the singular value decomposition. The Journal of the Astronautical Sciences **36**(3), 245–258 (1988)
11. Nguyen, V., Martinelli, A., Tomatis, N., Siegwart, R.: A comparison of line extraction algorithms using 2d laser rangefinder for indoor mobile robotics. In: International Conference on Intelligent Robots and Systems (IROS), pp. 1929–1934. IEEE (2005)
12. Pavlidis, T., Horowitz, S.L.: Segmentation of plane curves. IEEE transactions on Computers **23**(8), 860–870 (1974)
13. Shapiro, L., Stockman, G.C.: Computer vision. 2001. ed: Prentice Hall (2001)
14. Teixidó, M., Pallejà, T., Font, D., Tresanchez, M., Moreno, J., Palacín, J.: Two-dimensional radial laser scanning for circular marker detection and external mobile robot tracking. Sensors **12**(12), 16,482–16,497 (2012)
15. Thrun, S., Fox, D., Burgard, W., Dellaert, F.: Robust Monte Carlo localization for mobile robots. Artificial Intelligence **128**(1-2), 99–141 (2001)
16. Tice, B.P.: Unmanned aerial vehicles - the force multiplier of the 1990s. Airpower Journal (1991)
17. Wu, C.: Towards linear-time incremental structure from motion. In: International Conference on 3D Vision-3DV, IEEE, pp. 127–134 (2013)